Journal of Molecular Catalysis A: Chemical 324 (2010) 127–132

Contents lists available at ScienceDirect

Journal of Molecular Catalysis A: Chemical

journal homepage: www.elsevier.com/locate/molcata

Computational catalysis

Origin of enantioselectivity in asymmetric Pauson–Khand reactions catalyzed by [(BINAP)$Co_2(CO)_6$]☆

Torstein Fjermestad[a], Miquel A. Pericàs[a,b,*], Feliu Maseras[a,c,*]

[a] Institute of Chemical Research of Catalonia (ICIQ), Av Països Catalans 16, 43007 Tarragona, Spain
[b] Departament de Química Orgànica, Universitat de Barcelona, 08028 Barcelona, Spain
[c] Departament de Química, Universitat Autònoma de Barcelona, 08193 Bellaterra, Spain

ARTICLE INFO

Article history:
Available online 9 March 2010

Keywords:
Pauson–Khand reaction
Enantioselectivity
QM/MM methods

ABSTRACT

The quantum mechanics/molecular mechanics (QM/MM) ONIOM(B3LYP:UFF) approach is applied to the study of the asymmetric carbonylative intramolecular cycloaddition of a HCC–CH_2–N(Ts)–CH_2–CH=CH_2 enyne (Ts = tosyl) catalyzed by [(BINAP)$Co_2(CO)_6$] (BINAP = (1,1′-binaphtalene)-2,2′,diylbis(diphenylphosphine)). The experimental results, showing formation of the R product when the S-BINAP ligand is used, are reproduced. Comparison of the structures of the computed transition states leading to the R and S products provides a qualitative explanation for the origin of selectivity based on steric repulsions between specific substituents.

1. Introduction

The Pauson–Khand reaction (PKR), first introduced in the early seventies [1], has become one of the most powerful strategies for the construction of five-membered rings from simple precursors (Fig. 1) [2].

The original procedure, involving the use of stoichiometric amounts of cobalt precursors has been complemented with time with versions involving different metals [3], and intense research efforts have been devoted to the development of catalytic versions of the reaction [4]. The maturity of this methodology is clearly indicated by its routine use as the key step in the total synthesis of complex molecules [5]. In this context, the need for efficient synthetic procedures leading to enantiopure targets with known configuration has boosted research aimed at the development of enantioselective versions of the Pauson–Khand cyclopentenone synthesis [6]. Among them, the methodology developed by Gibson et al. for the catalytic and enantioselective intramolecular PKR, based on the use of a preformed complex obtained from [$Co_4(CO)_{12}$] and (S)-BINAP appears as one of the most promising alternatives [7].

Tha pre-catalyst in this approach, a [(BINAP)$Co_2(CO)_6$] species, presents the C_2 symmetric, bidentate ligand bonded to a single cobalt atom (Fig. 2), and it has been suggested that the whole reaction sequence takes place at the unsubstituted cobalt atom. According to this picture, the stereochemical course at the reaction is efficiently controlled by an otherwise spectator ligand.

A clear understanding of the catalytic cycle involved in this approach and of the factors controlling the stereochemical outcome of the reaction could play a fundamental role in the design of alternative ligands inducing high TON numbers and improved enantioselectivities in the reaction. With this ultimate goal, we decided to perform a theoretical study of the reaction mechanism likely operating in this transformation. Computational methods have been shown to be efficient for the study of enantioselective processes [8–10]. For this case, we applied QM/MM methods, especially appropriate for complexes containing bulky conformationally flexible ligands [11].

It is to be mentioned that the mechanism of the *normal* PKR, involving a dicobalt hexacarbonyl complex of an alkyne as starting material, has been scrutinized from the theoretical point of view [12], and different aspects of the reaction have found convincing explanation in this manner [13]. In addition, some PK-type reactions involving mononuclear complexes of iron [14], rhodium [15], and ruthenium [16] have been studied using DFT methodology; however, the Pauson–Khand reaction not involving the initial formation of an [(alkyne)$Co_2(CO)_6$] complex has remained completely unexplored from this perspective.

2. Computational details

The calculations were carried out using the Gaussian 03 program package [17]. The method used for the energy evaluations

☆ This paper is part of a special issue on Computational Catalysis.

* Corresponding authors at: Institute of Chemical Research of Catalonia (ICIQ), Av Països Catalans 16, 43007 Tarragona, Spain. Tel.: +34 977920202; fax: +34 977920231.
E-mail addresses: mapericas@iciq.es (M.A. Pericàs), fmaseras@iciq.es (F. Maseras).

1381-1169/$ – see front matter © 2010 Elsevier B.V. All rights reserved.
doi:10.1016/j.molcata.2010.03.006

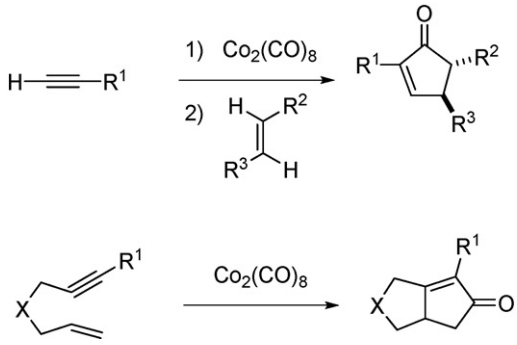

Fig. 1. Intermolecular (top) and intramolecular (bottom) versions of the Pauson–Khand reaction.

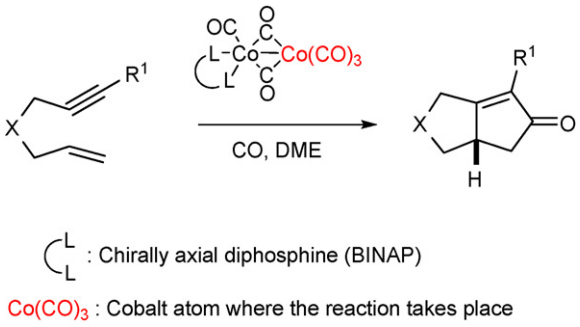

Fig. 2. Catalytic enantioselective Pauson–Khand reactions mediated by a preformed $[(BINAP)Co_2(CO)_6]$ species.

was ONIOM(B3LYP:UFF) [18–20]. The partition between the QM and MM regions used in most of the calculations is that of ONIOM partition 1 shown in Fig. 3. The basis set for the non-metal atoms was 6-31G(d) [21]. For the Co atoms, the core electrons were substituted by the Los Alamos effective core potential and the associated double zeta basis set was used for the valence electrons [22]. All minima and transition states were fully optimized without symmetry restrictions. The minima were identified by having only positive eigenvalues in the Hessian matrix whereas the transition states were identified by having a Hessian matrix with exactly one negative eigenvalue. All energies reported are Gibbs free energies, including zero-point and entropy corrections. In the selected cases where single-point QM calculations were carried out on the full system, the free energy corrections were taken from the corresponding ONIOM calculation. No solvation effects were considered because we assumed that they would not be critical in discriminating between pathways going to the R and S products. The calculation of enantiomeric excess relies in assuming that the ratio of products corresponds to a Boltzmann distribution of the relative energies of the key transition states leading to each of the products.

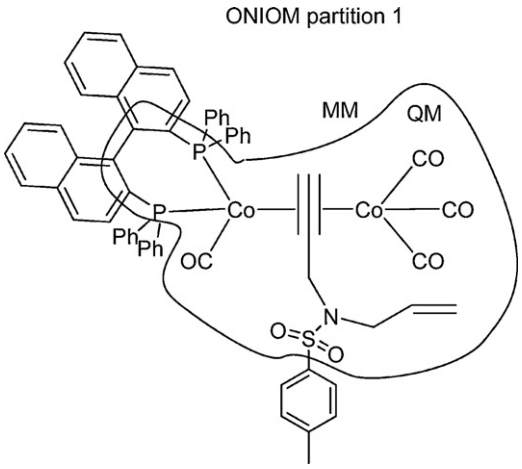

Fig. 3. Partition 1 between the QM and MM regions used in most of the calculations reported.

3. Results and discussion

3.1. Identification of the key transition state

The mechanism for the cobalt-catalyzed Pauson–Khand reaction has been previously characterized by computational studies, but only for the case of the intermolecular reaction of alkene and alkyne with $[Co_2(CO)_6]$ as metal complex [13]. The accepted mechanism is summarized in Fig. 4. In the initial adduct **ADD1**, the alkyne is coordinated to the complex after having displaced two bridging carbonyl groups of the $[Co_2(CO)_8]$ precursor. The steps of the process are then CO/alkene ligand exchange, oxidative metallacycle formation, CO insertion and reductive elimination. The highest energy transition state for the process, which we will label as **TS1**, corresponds to the conversion from **ADD2** to **INT1**. This is also the step where the C–C bond will be formed in the process we are studying, so it is a good candidate to control the enantioselectivity. Before concentrating on this particular step we had however to analyze the profile for the system under study.

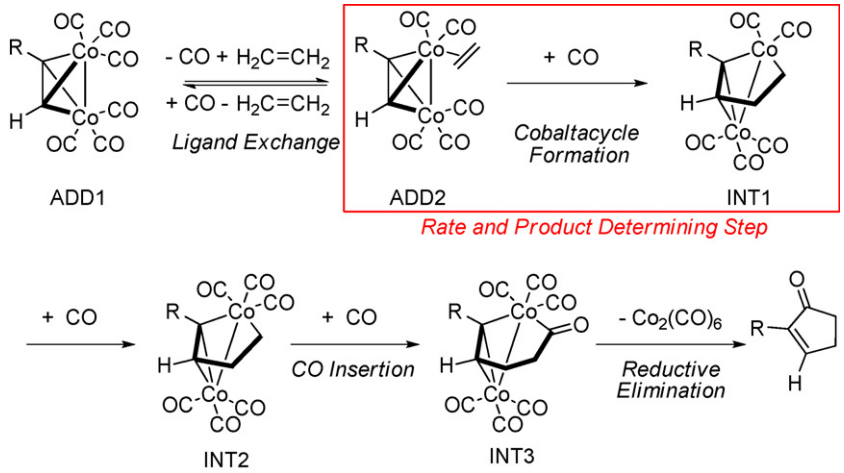

Fig. 4. Generally accepted mechanism for the dicobalt-catalyzed Pauson–Khand reaction.

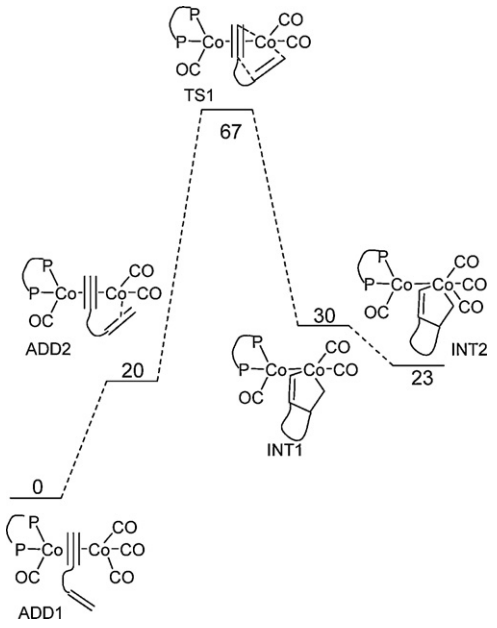

Fig. 5. Computed ONIOM(B3LYP:UFF) profile for the reaction under study.

The [(BINAP)$Co_2(CO)_4$] plus enyne system differs from the previously computed models in the presence of the BINAP ligand in the metal complex and in the presence of the linker connecting the alkene and alkyne units. This could bring qualitative changes to the energy profile. We computed part of the profile described in Fig. 4 for this system. The results are presented in Fig. 5. We focused on the transformation from **ADD1** to **INT2**. In these steps, the bond filling the coordination sphere of the new carbon stereogenic center is formed, and thus the enantioselectivity of the whole process is decided. The highest energy point of this profile is obviously TS1, which is thus confirmed as the key transition step in the process. We will analyze in the sections that follow the possible configurations of this key transition state leading to the R and the S products.

3.2. Four possible manifolds

The adduct from which the oxidative metallacycle formation starts, **ADD2**, can be in four different configurations. Each of these adducts will produce a manifold of pathways, that must be in principle studied, if we assume that the adducts are readily interconverted through fluxional processes [23] (Curtin–Hammett conditions). The structures of the four adducts are shown in Fig. 6.

The adduct leading to manifold A is the closest to the experimentally reported X-ray structure [7b], and because of this it was used in the free energy profile reported in the previous Section. The two phosphorus atoms of BINAP coordinate to the same cobalt center. One of the phosphorus occupies the axial position (towards the reader in the drawing), while the other is in one of the equatorial positions. The alkyne is coordinated with the linker pointing away from the equatorial phosphine. We assume, from the experimental data, that the arrangement of the BINAP ligand occupying the axial and one of the equatorial positions of one of the cobalt centers is the most stable one. This leaves however still other possibilities. In manifold B, the phosphorus coordinates in the other available equatorial position. Manifolds A and B are not equivalent because of the presence of a stereogenic center in BINAP. Manifolds C and D differ from the other two in the position of the alkene substituent, which is at the same side of the equatorial phosphorus center.

Direct experimental evidence from X-ray diffraction [7b] indicates the presence of an adduct related to manifold A, in equilibrium with a minor amount of an adduct related to manifold C, with the same BINAP arrangement. However, additional NMR evidence indicates that the two phosphorus centers have equivalent signals [7b], suggesting some type of equilibration mechanism that makes likely

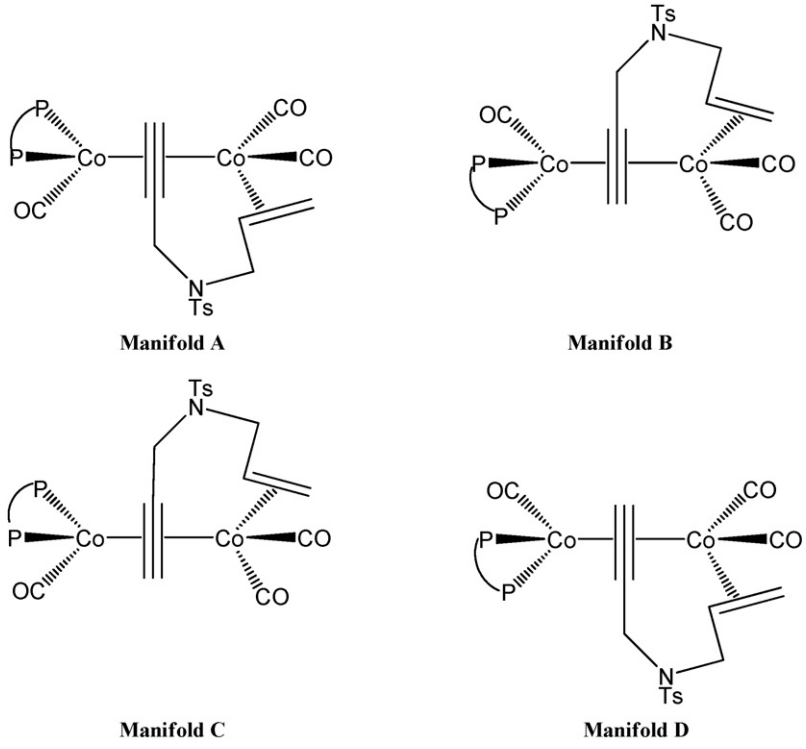

Fig. 6. Four possible structures for adduct **ADD2** leading to four different reaction manifolds.

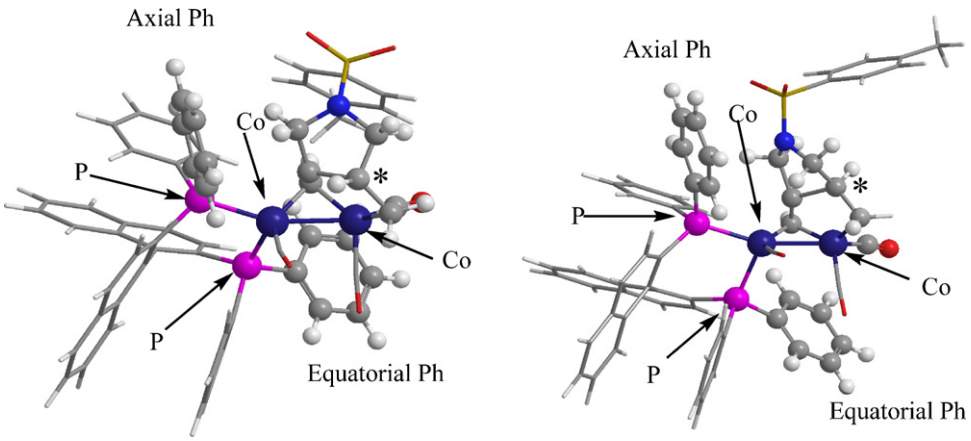

Fig. 7. ONIOM(B3LYP:UFF) optimized structures of transition states **A3** (left) and **A8** (right). Sterically relevant groups are highlighted by a ball-and-stick representation, and the newly created stereogenic center is marked with a star.

the easy accessibility of the four possible adducts in the experimental conditions.

3.3. Selectivity within manifold A

There are several possible conformations for the key transition state even when the research is constrained to a single manifold. A systematic conformational search was carried out by using three criteria: (i) the absolute configuration of the new stereogenic center (R or S), (ii) the absolute configuration at the nitrogen center (R or S) and (iii) the orientation of the torsion around the N–S bond (three possible staggered arrangements). The application of the three criteria results in twelve possible conformers for the transition state, that were systematically searched. Of these twelve conformers, labeled **A1** to **A12**, six became redundant by collapsing into each other. Of the six valid saddle points, four lead to the R product, **A1**, **A2**, **A3**, and **A6**, with relative energies of 5, 7, 0 and 6 kJ/mol. **A3**, which is the lowest energy saddle point, will be used from now on as origin of energies. The two saddle points leading to the S product, **A8**, **A9**, had relative energies of 9 and 11 kJ/mol, respectively. At a temperature of 348 K, this energy distribution of the transition states would lead to an enantiomeric excess of 92% in favor of the R product, in reasonable agreement with the experimental result of 88% ee [7a].

Fig. 7 presents the most stable structures of the saddle points leading to the R and S products from this manifold. In **A3**, the R conformation of the newly formed stereogenic center is indicated by the hydrogen attached to this atom pointing to the left. In contrast, in **A8**, it points to the right. **A3** is more stable than **A8** because there is less steric constraint in the ring being formed in this step. The ring is closer to planarity in **A3** than in **A8**, the average RMS deviation from the plane of the five atoms forming the ring being 0.260 Å in the former and 0.312 Å in the latter. The reason why this ring cannot be more planar in **A8** is because it would clash with the phenyl group labeled as "Axial Ph" in the drawing. The same type of reasoning is valid to discriminate between all R and S transition states for this manifold. Therefore, manifold A would produce as major product the R enantiomer.

3.4. Selectivity within other manifolds

Manifold B is particularly intriguing, because it should produce the S product by the same reasons that manifold A produces the R product. This was confirmed by a set of calculations on selected B transition states. The lowest energy transition states leading to the R and S products, respectively, were in this case **B8** and **B6**. And **B6** was indeed 6 kJ/mol below **B8**. The structures are shown in Fig. 8, and the five-membered ring being formed is more planar for **B6** (RMS deviation 0.253 Å) than for **B8** (RMS deviation 0.292 Å). The structures resulting from manifold B however have a higher energy than those resulting from manifold A. The relative energies of **B6**, **B8** with respective to **A3** are 13 and 19 kJ/mol, respectively. There-

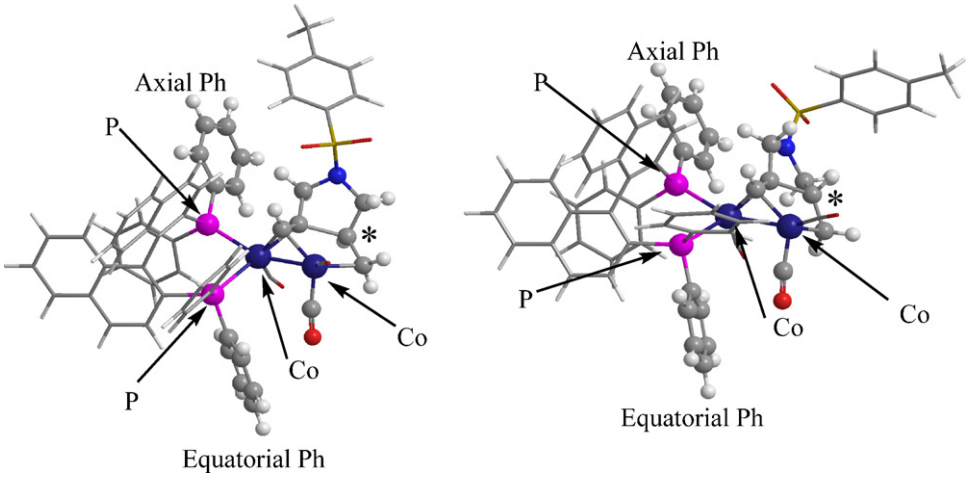

Fig. 8. ONIOM(B3LYP:UFF) optimized structures of transition states **B6** (left) and **B8** (right). Sterically relevant groups are highlighted by a ball-and-stick representation, and the newly created stereogenic center is marked with a star.

Table 1
Relative free energies (referred to **A3**, kJ/mol) of the conformers of **TS1** within the A manifold obtained with the different ONIOM partitions, as well with a single-point QM calculation.

Conformer	Associated product	Partition 1	Partition 2	Partition 3	Full QM
A1	R	5	−3	−1	−2
A2	R	7	6	−2	−3
A3	R	0	0	0	0
A6	R	7	4	−3	−4
A8	S	9	22	12	11
A9	S	11	9	17	16

fore, they do not affect critically the enantiomeric excess calculated exclusively from the relative energies of the transition states in manifold A (see above).

The difference between manifolds A and B is related to the stereogenic features of the BINAP ligand. The BINAP backbone puts a stronger steric constrain on one of the phenyl rings of each phosphorus center. These are the phenyl rings highlighted with a ball-and-stick representation in Figs. 7 and 8. The labels "axial" and "equatorial" refer in this case to the position occupied by the corresponding phosphorus atom in the cobalt coordination sphere. The steric role of the axial phenyl seems quite similar in both manifolds, but the difference in the steric effect of the equatorial phenyl is critical. In manifold A (Fig. 7) it points towards the back of the molecule, in a region without any obvious steric hindrance. The shortest contact between the critical carbonyl oxygen and the phenyl carbons is 3.315 Å in **A3** and 3.515 Å in **A8**. In manifold B, this phenyl points down, and the closest contacts are 3.137 Å in **B6** and 3.014 Å in **B8**. The higher energy of manifold B, that is necessary for the enantioselectivity of the whole process, is therefore related to the presence of a steric repulsion in a region far from that where the carbon–carbon is formed. The enantiomeric control takes place therefore by a mechanism different from that reported when monodentate chiral phosphines were applied in the Pauson–Khand reaction [6g,h].

Manifolds C and D were found to be not productive for this process because of steric hindrance. The side with the equatorial phosphorus is too crowded for the cyclometalation to take place. As a result, most of the transition state searches failed. We managed in any case to find to representative transition states, **C1** and **D1**, that are collected in the Supporting Information, and have energies of 29 and 49 kJ/mol above **A3**, respectively.

3.5. Validation of the computational approach

The partition between QM and MM regions is a critical point in the validity of the applied computational approach. Because of this, we carried out a series of supplementary calculations with larger QM regions for the case of manifold A. These new QM/MM partitions are labeled as partition 2 and partition 3. In partition 1 (Fig. 3), the MM region consisted of the naphthyl rings in BINAP, the phenyl rings on the phosphorus centers, and the tolyl in the tosyl group. In partition 2, the phenyl rings are moved to the QM region. In partition 3, the tolyl group is also moved to the QM region, and only the naphthyl rings in BINAP remain the MM region.

The six conformers of **TS1** within manifold A reported in the previous sections were fully reoptimized with partitions 2 and 3. All of them happened to exist as saddle points also with the two new partitions. Their relative energies are summarized in Table 1. The results are not optimal, in the sense that the relative energies change with the partition. The most demanding ONIOM partition 3 provides a sufficiently accurate description, because differences with respect to single-point B3LYP calculations on the full system reported in the last column are of 1 kJ/mol at most. The changes between partitions can be attributed either to a poor reproduction of non-bonding interactions by the UFF force field [24] or to the neglection of electronic effects by the MM description [25,26]. However, the qualitative picture concerning enantioselectivity is unchanged: the conformers leading to the R enantiomer are always below those leading to the S enantiomer. Therefore, our more economic partition 1 is able to provide a reliable qualitative picture and explain why one product is formed over the other. A more accurate method would be required to obtain quantitatively reliable predictions of enantiomeric excess, but this would be again very challenging given the small energy differences involved.

4. Conclusions

Our computational study on the Pauson–Khand reaction of the HCC–CH_2–N(Ts)–CH_2–CH=CH_2 enyne catalyzed by [(BINAP)$Co_2(CO)_6$] succeeds in reproducing the experimentally observed formation of the R product when the S-BINAP ligand is used. The key transition state determining the enantioselectivity corresponds to the oxidative cyclometalation step. A variety of possible structures are available for this transition state, some leading to the R product, and some leading to the S product. The grouping of these structures in manifolds depending on the enyne–dicobalt complex they derive from allows for a simple explanation of the observed behavior. The energy ordering between the manifolds is decided by the chirality of the BINAP ligand. The S form of the BINAP ligand favors the manifold we have labeled as A because of a reduced steric repulsion between the BINAP phenyl groups and the carbonyl groups attached to the other cobalt center. Within a given manifold, the nature of the product is determined by steric repulsions between the linker group in the enyne and the BINAP substituents. The A manifold favors the R product, which is thus the experimentally observed. The minor S product could be formed from either the less favorable transition state conformers of this manifold or from the most favored transition state conformers of the alternative manifold B.

The application of the QM/MM approach ONIOM to this experimental problem illustrates the high potential of this approach to gain insight into complex enantioselectivity problems with a reasonable computer effort. This work also proves however the limitations of the method in the sense that more accurate results could be obtained with consideration of a larger QM region or consideration of a full QM approach.

Acknowledgments

We thank MICINN (projects CTQ2008-00947-BQU, CTQ2008-06866-CO2-02 and Consolider Ingenio 2010 grant CSD2006-0003), Generalitat de Catalunya (grants 2009SGR0259 and 2009SGR0623) and the ICIQ foundation for financial support.

This work was funded by the Deutsche Forschungsgemeinschaft, grant no. 1208/6.

Appendix A. Supplementary data

Supplementary data associated with this article can be found, in the online version, at doi:10.1016/j.molcata.2010.03.006.

Cartesian coordinates, total energies and imaginary frequencies for all optimized structures.

References

[1] I.U. Khand, G.R. Knox, P.L. Pauson, W.E. Watts, M.I. Foreman, J. Chem. Soc., Perkin Trans. I (1973) 977–981.
[2] For some recent reviews, see:
(a) D. Struebing, M. Beller, Top. Organomet. Chem. 18 (2006) 165–178;
(b) T. Shibata, Adv. Synth. Catal. 348 (2006) 2328–2336;
(c) S. Laschat, A. Becheanu, T. Bell, A. Baro, Synlett (2005) 2547–2570;

(d) S.E. Gibson, N. Mainolfi, Angew. Chem. Int. Ed. 44 (2005) 3022–3037;
(e) L.V.R. Bonaga, M.E. Krafft, Tetrahedron 60 (2004) 9795–9833.
[3] Titanium:
(a) F.A. Hicks, S.L. Buchwald, J. Am. Chem. Soc. 118 (1996) 11688–11689;
(b) S.J. Sturla, S.L. Buchwald, J. Org. Chem. 64 (1999) 5547–5550;
Iron:
(c) A.J. Pearson, R.A. Dubbert, Organometallics 13 (1994) 1656–1661;
Zirconium:
(d) E. Negishi, S.J. Holmes, J.M. Tour, J.A. Miller, J. Am. Chem. Soc. 107 (1985) 2568–2569;
Molibdenum:
(e) K.M. Brummond, A.D. Kerekes, H. Wan, J. Org. Chem. 67 (2002) 5156–5163;
(f) H. Cao, J. Flippen-Anderson, J.M. Cook, J. Am. Chem. Soc. 125 (2003) 3230–3231;
Ruthenium:
(g) T. Morimoto, N. Chatani, Y. Fukumoto, S. Murai, J. Org. Chem. 62 (1997) 3762–3765;
(h) T. Kondo, N. Suzuki, T. Okada, T. Mitsudo, J. Am. Chem. Soc. 119 (1997) 6187–6188;
Rhodium:
(i) Y. Koga, T. Kobayashi, K. Narasaka, Chem. Lett. (1998) 249–250;
(j) N. Jeong, Organometallics 17 (1998) 3642–3644;
Tungsten:
(k) T.R. Hoye, J.A. Suriano, Organometallics 11 (1992) 2044–2050;
(l) T.R. Hoye, J.A. Suriano, J. Am. Chem. Soc. 115 (1993) 1154–1156;
Iridium:
(m) T. Shibata, K. Takagi, J. Am. Chem. Soc. 122 (2000) 9852–9853.
[4] (a) V. Rautenstrauch, P. Megard, J. Conesa, W. Kuester, Angew. Chem. Int. Ed. 29 (1990) 1413–1416;
(b) N. Jeong, S.H. Hwang, Y. Lee, Y.K. Chung, J. Am. Chem. Soc. 116 (1994) 3159–3160, For a review devoted to this specific topic, see Ref. [2b].
[5] For recent examples, see:
(a) A. Nakayama, N. Kogure, M. Kitajima, H. Takayama, Org. Lett. 11 (2009) 5554–5557;
(b) Y. Hayashi, N. Miyakoshi, S. Kitagaki, C. Mukai, Org. Lett. 10 (2008) 2385–2388;
For Pioneering work, see:
(c) C. Exon, P. Magnus, J. Am. Chem. Soc. 105 (1983) 2477–2478;
(d) P. Magnus, C. Exon, P. Albaugh-Robertson, Tetrahedron 41 (1985) 5861–5869;
(e) D.H. Hua, J. Am. Chem. Soc. 108 (1986) 3835–3836.
[6] For stoichiometric approaches, see:
(a) J. Castro, H. Sörensen, A. Riera, C. Morin, A. Moyano, M.A. Pericàs, A.E. Greene, J. Am. Chem. Soc. 112 (1990) 9388–9389;
(b) M. Poch, E. Valentí, A. Moyano, M.A. Pericàs, J. Castro, A. DeNicola, A.E. Greene, Tetrahedron Lett. 31 (1990) 7505–7508;
(c) X. Verdaguer, A. Moyano, M.A. Pericàs, A. Riera, A.E. Greene, J.F. Piniella, A. Alvarez-Larena, J. Organomet. Chem. 433 (1992) 305–310;
(d) J. Castro, A. Moyano, M.A. Pericàs, A. Riera, A.E. Greene, Tetrahedron: Asymmetry 5 (1994) 307–310;
(e) X. Verdaguer, A. Moyano, M.A. Pericàs, A. Riera, V. Bernardes, A.E. Greene, A. Alvarez-Larena, J.F. Piniella, J. Am. Chem. Soc. 116 (1994) 2153–2154;
(f) V. Bernardes, N. Kann, A. Riera, A. Moyano, M.A. Pericàs, A.E. Greene, J. Org. Chem. 60 (1995) 6670–6671;
(g) J. Castro, A. Moyano, M.A. Pericàs, A. Riera, A. Alvarez-Larena, J.F. Piniella, J. Am. Chem. Soc. 122 (2000) 7944–7952;
(h) X. Verdaguer, A. Moyano, M.A. Pericàs, A. Riera, M.A. Maestro, J. Mahia, J. Am. Chem. Soc. 122 (2000) 10242–10243;
(i) X. Verdaguer, M.A. Pericàs, A. Riera, M.A. Maestro, J. Mahia, Organometallics 22 (2003) 1868–1877;
For catalytic approaches, see:
(j) F.A. Hicks, S.L. Buchwald, J. Am. Chem. Soc. 121 (1999) 7026–7033;
(k) K. Hiroi, T. Watanabe, R. Kawagishi, I. Abe, Tetrahedron Lett. 41 (2000) 891–895;
(l) K. Hiroi, T. Watanabe, R. Kawagishi, I. Abe, Tetrahedron: Asymmetry 11 (2000) 797–808;
(m) S.J. Sturla, S.L. Buchwald, J. Org. Chem. 67 (2002) 3398–3403.
[7] (a) S.E. Gibson, S.E. Lewis, J.A. Loch, J.W. Steed, M.J. Tozer, Organometallics 22 (2003) 5382–5384;
(b) S.E. Gibson, K.A.C. Kaufmann, J.A. Loch, J.W. Steed, A.J.P. White, Chem. Eur. J. 11 (2005) 2566–2576;
(c) S.E. Gibson, D.J. Hardick, P.R. Haycock, K.A.C. Kaufmann, A. Miyazaki, M.J. Tozer, A.J.P. White, Chem. Eur. J. 13 (2007) 7099–7109.
[8] (a) D. Balcells, F. Maseras, New J. Chem. 31 (2007) 333–343;
(b) J.M. Brown, R.J. Deeth, Angew. Chem. Int. Ed. 48 (2009) 4476–4479.
[9] (a) G. Ujaque, F. Maseras, A. Lledos, J. Am. Chem. Soc. 121 (1999) 1317–1323;
(b) J. Vazquez, M.A. Pericas, F. Maseras, A. Lledos, J. Org. Chem. 65 (2000) 7303–7309;
(c) D. Balcells, F. Maseras, G. Ujaque, J. Am. Chem. Soc. 127 (2005) 3624–3634.
[10] (a) S. Feldgus, C.R. Landis, J. Am. Chem. Soc. 122 (2000) 12714–12727;
(b) J. Rudolph, C. Bolm, P.-O. Norrby, J. Am. Chem. Soc. 127 (2005) 1548–1552.
[11] (a) G. Ujaque, F. Maseras, Struct. Bond 112 (2004) 117–149;
(b) C. Bo, F. Maseras, Dalton Trans. (2008) 2911–2919.
[12] (a) M. Yamanaka, E. Nakamura, J. Am. Chem. Soc. 123 (2001) 1703–1708;
(b) M.A. Pericàs, J. Balsells, J. Castro, I. Marchueta, A. Moyano, A. Riera, J. Vázquez, X. Verdaguer, Pure Appl. Chem. 74 (2002) 167–174.
[13] (a) X. Verdaguer, J. Vazquez, G. Fuster, V. Bernardes-Genisson, A.E. Greene, A. Moyano, M.A. Pericàs, A. Riera, J. Org. Chem. 63 (1998) 7037–7052;
(b) J. Balsells, J. Vazquez, A. Moyano, M.A. Pericàs, A. Riera, J. Org. Chem. 65 (2000) 7291–7302;
(c) T.J.M. De Bruin, A. Milet, F. Robert, Y. Gimbert, A.E. Greene, J. Am. Chem. Soc. 123 (2001) 7184–7185;
(d) T.J.M. De Bruin, A. Milet, A.E. Greene, Y. Gimbert, J. Org. Chem. 69 (2004) 1075–1080;
(e) C.P. del Valle, A. Milet, Y. Gimbert, A.E. Greene, Angew. Chem. Int. Ed. 44 (2005) 5717–5719;
(f) T.J.M. De Bruin, C. Michel, K. Vekey, A.E. Greene, Y. Gimbert, A. Milet, J. Organomet. Chem. 691 (2006) 4281–4288.
[14] W. Imhof, E. Anders, A. Göbel, H. Görls, Chem. Eur. J. 9 (2003) 1166–1181.
[15] W.H. Pitcock, R.L. Lord, M.-H. Balk, J. Am. Chem. Soc. 130 (2008) 5821–5830.
[16] C. Wang, Y.-D. Wu, Organometallics 27 (2008) 6152–6162.
[17] M.J. Frisch, G.W. Trucks, H.B. Schlegel, G.E. Scuseria, M.A. Robb, J.R. Cheeseman, J.A. Montgomery Jr., T. Vreven, K.N. Kudin, J.C. Burant, J.M. Millam, S.S. Iyengar, J. Tomasi, V. Barone, B. Mennucci, M. Cossi, G. Scalmani, N. Rega, G.A. Petersson, H. Nakatsuji, M. Hada, M. Ehara, K. Toyota, R. Fukuda, J. Hasegawa, M. Ishida, T. Nakajima, Y. Honda, O. Kitao, H. Nakai, M. Klene, X. Li, J.E. Knox, H.P. Hratchian, J.B. Cross, V. Bakken, C. Adamo, J. Jaramillo, R. Gomperts, R.E. Stratmann, O. Yazyev, A.J. Austin, R. Cammi, C. Pomelli, J.W. Ochterski, P.Y. Ayala, K. Morokuma, G.A. Voth, P. Salvador, J.J. Dannenberg, V.G. Zakrzewski, S. Dapprich, A.D. Daniels, M.C. Strain, O. Farkas, D.K. Malick, A.D. Rabuck, K. Raghavachari, J.B. Foresman, J.V. Ortiz, Q. Cui, A.G. Baboul, S. Clifford, J. Cioslowski, B.B. Stefanov, G. Liu, A. Liashenko, P. Piskorz, I. Komaromi, R.L. Martin, D.J. Fox, T. Keith, M.A. Al-Laham, C.Y. Peng, A. Nanayakkara, M. Challacombe, P.M.W. Gill, B. Johnson, W. Chen, M.W. Wong, C. Gonzalez, J.A. Pople, Gaussian 03, Revision C.02, Gaussian Inc., Wallingford, CT, 2004.
[18] (a) F. Maseras, K. Morokuma, J. Comput. Chem. 16 (1995) 1170–1179;
(b) M. Svensson, S. Humbel, R.D.J. Froese, T. Matsubara, S. Sieber, K. Morokuma, J. Phys. Chem. 100 (1996) 19357–19363.
[19] (a) A.D. Becke, J. Chem. Phys. 98 (1993) 5648–5652;
(b) C.T. Lee, W.T. Yang, R.G. Parr, Phys. Rev. B 37 (1988) 785–789.
[20] A.K. Rappé, C.J. Casewit, K.S. Colwell, W.A. Goddard III, W.M. Skiff, J. Am. Chem. Soc. 114 (1992) 10024–10035.
[21] R. Ditchfield, W.J. Hehre, J.A. Pople, J. Chem. Phys. 54 (1971) 724–728.
[22] P.J. Hay, W.R. Wadt, J. Chem. Phys. 82 (1985) 270–283.
[23] (a) S. Aime, L. Milone, R. Rossetti, P.L. Stanghellini, Inorg. Chim. Acta 22 (1977) 135–139;
(b) E. Band, E.L. Muetterties, Chem. Rev. 78 (1978) 639–658.
[24] D. Balcells, G. Drudis-Solé, M. Besora, N. Dölker, G. Ujaque, F. Maseras, A. Lledós, Faraday Discuss 124 (2003) 429–441.
[25] S.M.A. Donald, A. Vidal-Ferran, F. Maseras, Can. J. Chem. 87 (2009) 1273–1279.
[26] V.P. Ananikov, D.G. Musaev, K. Morokuma, Eur. J. Inorg. Chem. 34 (2007) 5390–5399.